Journal of Alloys and Compounds 491 (2010) 753–760

Contents lists available at ScienceDirect

Journal of Alloys and Compounds

journal homepage: www.elsevier.com/locate/jallcom

Effect of molybdenum addition on metastability of cubic γ-uranium

V.P. Sinha[a,*], P.V. Hegde[a], G.J. Prasad[a], G.K. Dey[b], H.S. Kamath[a]

[a] Metallic Fuels Division, Bhabha Atomic Research Centre, Mumbai 400085, India
[b] Material Science Division, Bhabha Atomic Research Centre, Mumbai 400085, India

ARTICLE INFO

Article history:
Received 16 July 2009
Accepted 7 November 2009
Available online 13 November 2009

Keywords:
Phase
Dispersoid
Powder
Matrix
Alloy
Microstructure

ABSTRACT

Over the years U_3Si_2 compound dispersed in aluminium matrix has been used successfully as the potential low enriched uranium (LEU < 20%U^{235}) base dispersion fuel for use in new research and test reactors and also for converting high enriched uranium (HEU > 85%U^{235}) cores to LEU for most of the existing research and test reactors world over, though maximum 4.8 g U cm^{-3} density is achievable with U_3Si_2–Al dispersion fuel. To achieve a uranium density of 8.0–9.0 g U cm^{-3} in dispersion fuel with aluminium as matrix material, it is required to use γ-stabilized uranium metal powders. At Bhabha Atomic Research Centre (BARC), R & D efforts are on to develop these high density uranium base alloys. This paper describes the alloying behaviour of uranium with varying amount of molybdenum. The U–Mo alloys with different molybdenum content have been prepared by using an induction melting furnace with uranium and molybdenum metal pellets as starting materials. U–Mo alloys with different molybdenum content were characterized by X-ray diffraction (XRD) for phase identification and lattice parameter measurements. The optical microstructure of different U–Mo alloy composition has also been discussed in this paper. Quantitative image analysis was also carried out to determine the amount of various phases in each composition.

© 2009 Elsevier B.V. All rights reserved.

1. Introduction

In 1978 the US programme on reduced enrichment for research and test reactors (RERTR) was initiated with the sole objective of converting high enriched uranium (HEU > 85%U^{235}) core for the existing research and test reactors world over to low enriched uranium (LEU < 20%U^{235}) core due to the concerns on nuclear proliferation and diversion [1]. After this the nuclear fuel designers have to develop a fuel cycle based on LEU rather than HEU which indirectly means either one has to increase the fuel loading in the meat or develop high density uranium compounds/alloys to compensate the lower uranium enrichment. With CERCA's experience of highly loaded U_3Si_2–Al and UN–Al fuels it was shown that the fuel volume loading of greater than 55 vol% was not achievable in a commercially viable process with fuel dispersants of very high uranium density (i.e. >15 g U cm^{-3}) [2,3]. Due to limitation on the increase of fuel particle volume fraction in the fuel meat the only other option is to increase the heavy metal (i.e. uranium) density of the fuel itself. This can be achieved by using high density uranium compounds or alloys as fuels. In 1987, the fuel development programme for RERTR was joined by many other countries which gave an impetus on the cooperative research and development work on LEU fuels. This resulted in the successful development and qualification of some uranium compounds of higher heavy metal density for dispersion fuel application (i.e. U_3O_8–Al at 3.2 g U cm^{-3} and U_3Si_2–Al at 4.8 g U cm^{-3}). It was realized by then that 4.8 g U cm^{-3} of uranium density in the fuel is sufficient to convert most of the existing research and test reactors cores of HEU in LEU, without making any alteration in the reactor design. Still higher uranium density fuel compounds/alloys are required to be developed to fulfill the objective of fuel designers to develop a fuel system which can achieve a heavy metal density of 8–9 g U cm^{-3} since many of the researchers wanted to develop a neutron source with high thermal neutron flux density for superior quality experiments [4].

Several intermetallic compounds of uranium like U_3Si and U_6Me where Me can be Fe, Ni, Mn, Co or Ge were considered initially because of their higher heavy metal density (see Fig. 1). These compounds exhibit high swelling rate (break away swelling) even at relatively low burnups hence they were not considered further as potential ultra high density uranium dispersoids by the fuel designers [5–8]. Therefore, uranium metal density of the order of 8–9 g U cm^{-3} in the fuel meat can be achieved only with the use of pure uranium metal or uranium alloys as dispersoids. The room temperature phase of pure uranium (i.e. α-uranium having orthorhombic crystal structure) shows very poor irradiation stability (even under low burnups and high temperature irradiation

* Corresponding author at: MFD, NFG, Bhabha Atomic Research Centre, Trombay, Mumbai 400085, India. Tel.: +91 22 25590697.
E-mail address: vedsinha@barc.gov.in (V.P. Sinha).

0925-8388/$ – see front matter © 2009 Elsevier B.V. All rights reserved.
doi:10.1016/j.jallcom.2009.11.060

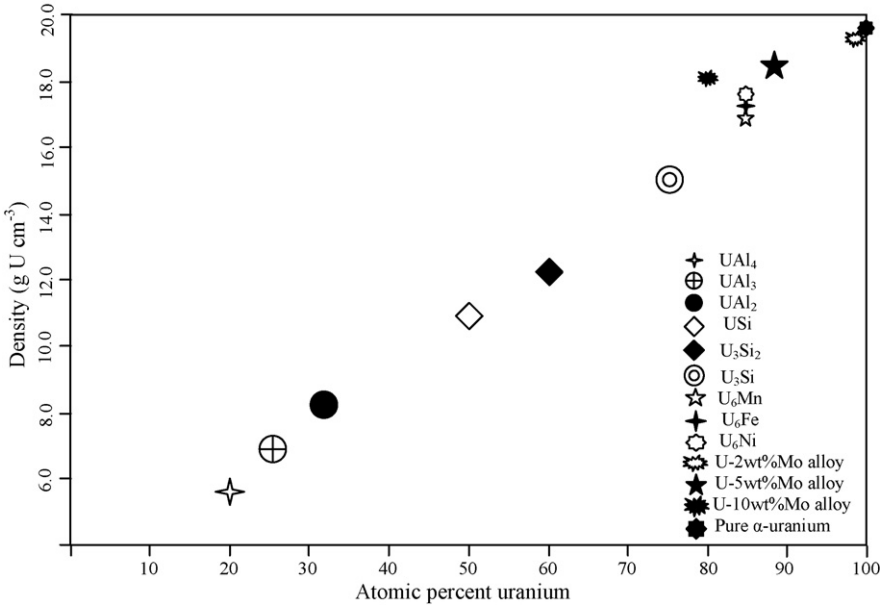

Fig. 1. Density of different uranium compounds/alloys.

conditions) due to cavitational swelling under irradiation and thermal growth under power ramping which makes it unsuitable as fuel [9]. On the other hand the high temperature phase of pure uranium (i.e. γ-uranium having body centered crystal structure) is quite stable under irradiation than α-uranium since swelling takes place mainly due to fission gas nucleation and growth mechanism here. Thermodynamically high temperature pure cubic γ-uranium is not stable under preparation and irradiation condition however there are some alloying elements which can make the high temperature pure γ-uranium metastable at room temperature. Several transition metals, particularly from Group IVA to Group VIIIA of periodic table form solid solution with γ-U, which can be retained as metastable phase at room temperature upon cooling. The stabilizing power of these elements increases with their atomic number since more and more d-electrons will participate in bonding due to hybridization with s and p orbital electrons. However, their solubility will decrease as the size difference with uranium atom increases. In fact the increase in bond strength with the increase in atomic number of transition elements will promote the formation of intermetallic compound rather than a solid solution. The alloys which have a tendency to form stable cubic phase of uranium at room temperature are U–Zr, U–Mo, U–Nb, U–Re, U–Ru, U–Ti, etc. [10]. The first two transition elements of 4d series (i.e. Zr and Nb) will form complete solid solution with γ-uranium but to retain the 100% γ-phase of uranium at room temperature, large concentration of these elements are required to be added in the alloy. On the other extreme Pd and Pt have only ~2 at% solubility in γ-uranium and these alloying elements will give very stable intermetallic compounds with uranium. It was earlier recognized that molybdenum is a good compromise for the two extremes mentioned above [11].

In uranium molybdenum system under equilibrium cooling, the cubic γ-phase with the space group *Im*3*m* will break into orthorhombic α-phase of space group *Cmcm* and body centered tetragonal γ′-phase (U_2Mo) of space group *I*4/*mmm* (see Fig. 2). However under rapid cooling conditions the metastable γ-phase can be retained at the room temperature. The U–Mo alloys containing less than 11 at% Mo when water quenched from the gamma phase region may be called as alpha phase alloys while those with more than 11 at% Mo may be called as gamma phase alloys under the same conditions [12–16]. In fact the U–Mo alloys containing up to 10 at% Mo when quenched in water forms α′ and α″ phases which are slight variation from the orthorhombic α-phase [17,18]. Tangri has reported base centered tetragonal phase γ° for water quenched alloys containing 11.39 at% to 12.73 at% Mo [19].

In connection with dispersion fuel development work at BARC, R & D efforts are on to develop high density uranium alloys/compounds to fulfill certain departmental objective [20,21] and also address the international concern on proliferation. Under this programme U–Mo alloys with different molybdenum contents have been prepared and characterized and the results are discussed in the paper. The U–Mo alloys were prepared in an induction furnace with uranium and molybdenum metal pieces as starting materials. U–Mo alloys of different compositions were then analyzed by XRD for phase and precise lattice parameter calculation and the results are included in the paper. Uranium and molybdenum forms substitutional solid solution with each other hence the effect of molybdenum addition to the lattice parameter of cubic γ-uranium has also been discussed. The precise lattice parameter calculation was done using CELREF programme. Optical microstructures of U–Mo alloys have been developed and discussed. Optical microstructures of various U–Mo alloys were then evaluated by image analysis for quantifying different phases present.

2. Experimental work

2.1. Alloy preparation

The starting materials for the purpose are cylindrical uranium metal pellets (shown in Fig. 3(a)) and molybdenum metal pieces (shown in Fig. 3(b)). Uranium metal pieces were having 99.9 wt% 'U-content' and molybdenum metal pieces were having 99.8 wt% 'Mo-content'. The uranium metal pellets used here were approximately of 12 mm diameter and around 10 mm in length while molybdenum metal pieces were cut in small disks of around 3.5 mm in diameter and 2 mm in height. Uranium metal pieces were then electropolished using orthophosphoric acid as electrolyte to remove any surface oxide layer. The electropolished uranium metal pieces and molybdenum metal disks were then ultrasonically cleaned.

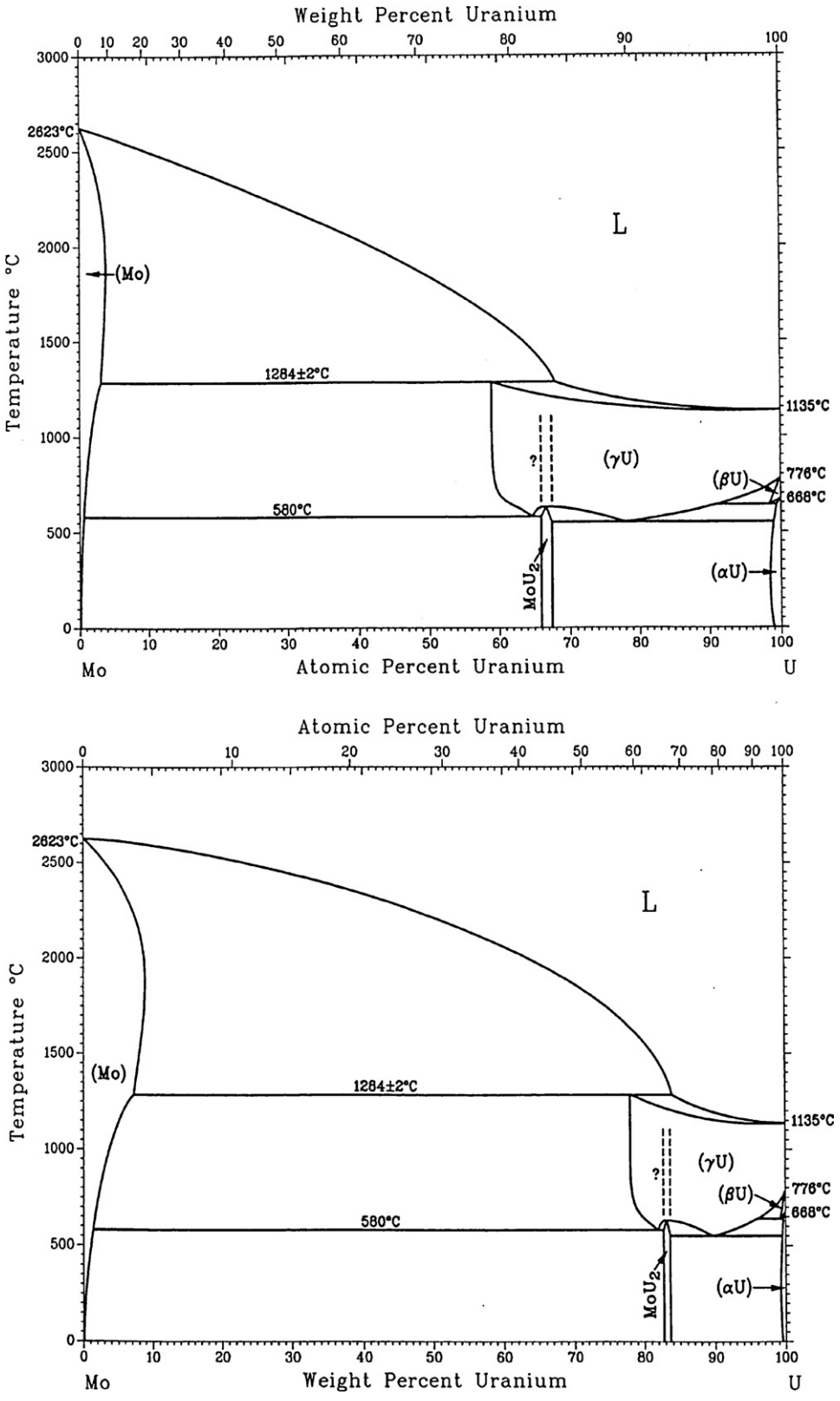

Fig. 2. Uranium–molybdenum phase diagram.

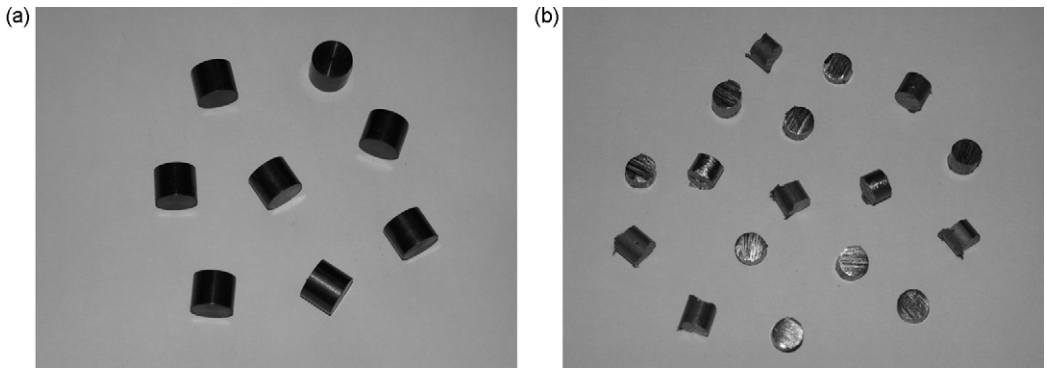

Fig. 3. Photograph of (a) uranium metal pellets and (b) molybdenum metal pieces.

Table 1
Weights of constituent elements and cast U–Mo alloys.

Composition of U–Mo alloy	Uranium weight (g)	Molybdenum weight (g)	U–Mo alloy weight (g)
U–2 wt%Mo	88.40	1.8	90.30
U–5 wt%Mo	61.20	3.22	64.44
U–6 wt%Mo	63.94	4.14	68.07
U–7 wt%Mo	64.89	4.90	69.78
U–8 wt%Mo	63.4	5.46	68.87
U–9 wt%Mo	64.79	6.41	71.24
U–10 wt%Mo	67.11	7.40	74.53

Uranium metal pellets and molybdenum metal pieces were then charged in yitria coated graphite crucible along with molybdenum metal pieces in required quantity for melting. The crucible was then loaded in an induction heating furnace and melting was done at $1300 \pm 10\,^{\circ}C$ for 30 min under vacuum of 10^{-5} mbar. The induction furnace was flushed thrice with high purity argon gas to remove traces of oxygen before melting. Melting was done at $1300\,^{\circ}C$ since the liquidous temperature of all the U–Mo alloys with different molybdenum content discussed in the present paper is around $1140 \pm 20\,^{\circ}C$. The furnace was then allowed to cool under vacuum and U–Mo alloy ingot was taken out. The ingot was then cleaned ultrasonically and weight was taken in a micro-balance. U–Mo alloys with seven different compositions (i.e. U–2 wt%Mo, U–5 wt%Mo, U–6 wt%Mo, U–7 wt%Mo, U–8 wt%Mo, U–9 wt%Mo and U–10 wt%Mo) have been prepared to study the effect of molybdenum addition on uranium and metastability of cubic γ-uranium. The U–Mo alloy ingots thus prepared were of typical dimension of around 15 mm diameter and 40 mm length. The final weight of all alloy ingots was recorded and is shown in Table 1.

2.2. Characterization

The XRD sample of alloys of different compositions were prepared by cutting the cast ingots in silicon carbide cut off wheel to get small disk of 15 mm diameter and 4 mm height. The disks were polished by 2 μm diamond paste in standard metallographic set up to get good surface finish. The polished samples were then scanned in standard theta–theta XRD equipment with a scan rate of $0.5^{\circ}\,min^{-1}$. Standard source of Cu Kα radiation with curved graphite monochromater and sealed proportional counter was used in the machine. Instrument was operated at 1 kW with tube voltage and tube current at 35.0 kV and 28.4 mA, respectively to generate XRD patterns for all the U–Mo alloys. Precise lattice parameter of each alloy was calculated by using CELREF programme.

The metallographic sample from each composition of U–Mo alloy was prepared by cold mounting the disk of 15 mm diameter and 4 mm height. Cold mounted samples were ground and polished by using standard metallography equipment and procedures. The polished samples were then etched by freshly prepared etchants.

Table 2
Description of etchants used for different U–Mo alloys.

Composition of alloy	Etchant composition and process details
U–2 wt%Mo, U–5 wt%Mo and U–6 wt%Mo	5 part orthophosphoric acid and 100 part H_2O. 2–2.5 V open circuit, stainless steel cathode is used for electrolytic etching
U–7 wt%Mo, U–8 wt%Mo, U–9 wt%Mo and U–10 wt%Mo	1 part orthophosphoric acid, 2 part H_2SO_4 and 2 part H_2O. Used as chemical etchant, freshly polished sample is attacked with few drops

Different etchants were used for different molybdenum alloy composition (see Table 2). Etched samples were then examined in Leica make, DMI5000M optical microscope. The microstructure of U–Mo alloy of different molybdenum content was evaluated by quantitative image analysis to determine the amount of various phases.

3. Results and discussion

In uranium molybdenum system under equilibrium cooling the body centered cubic γ-phase with the space group *Im*3*m* will break into orthorhombic α-phase with the space group *Cmcm* and body centered tetragonal intermetallic compound U_2Mo with the space group *I*4/*mmm*. A minimum of 33 at% of molybdenum is required for the formation of U_2Mo intermetallic compound which is possible only with the diffusion of molybdenum. Since the diffusivity of molybdenum is very slow the eutectoid reaction requires sufficient thermal activation energy and soaking time. The equilibrium cooling curve of U–Mo alloy will shift to the right with the addition of molybdenum which allows the retention of metastable cubic γ-phase at room temperature under normal cooling condition though in alloys with lower molybdenum content metastable cubic γ-phase of uranium can be retained at room temperature under rapid cooling (i.e. quenching) [10].

Table 3
Precise lattice parameter and lattice volume of orthorhombic α-uranium in U–Mo alloys.

Composition of alloy	Precise lattice parameter of α-uranium (Å)			Lattice volume (Å^3)
	a	*b*	*c*	
Unalloyed α-uranium at RT	2.8540	5.8700	4.9550	83.0110
U–2 wt%Mo	2.8603	5.8729	4.9560	83.2434
U–5 wt%Mo	2.8632	5.8741	4.9582	83.3906

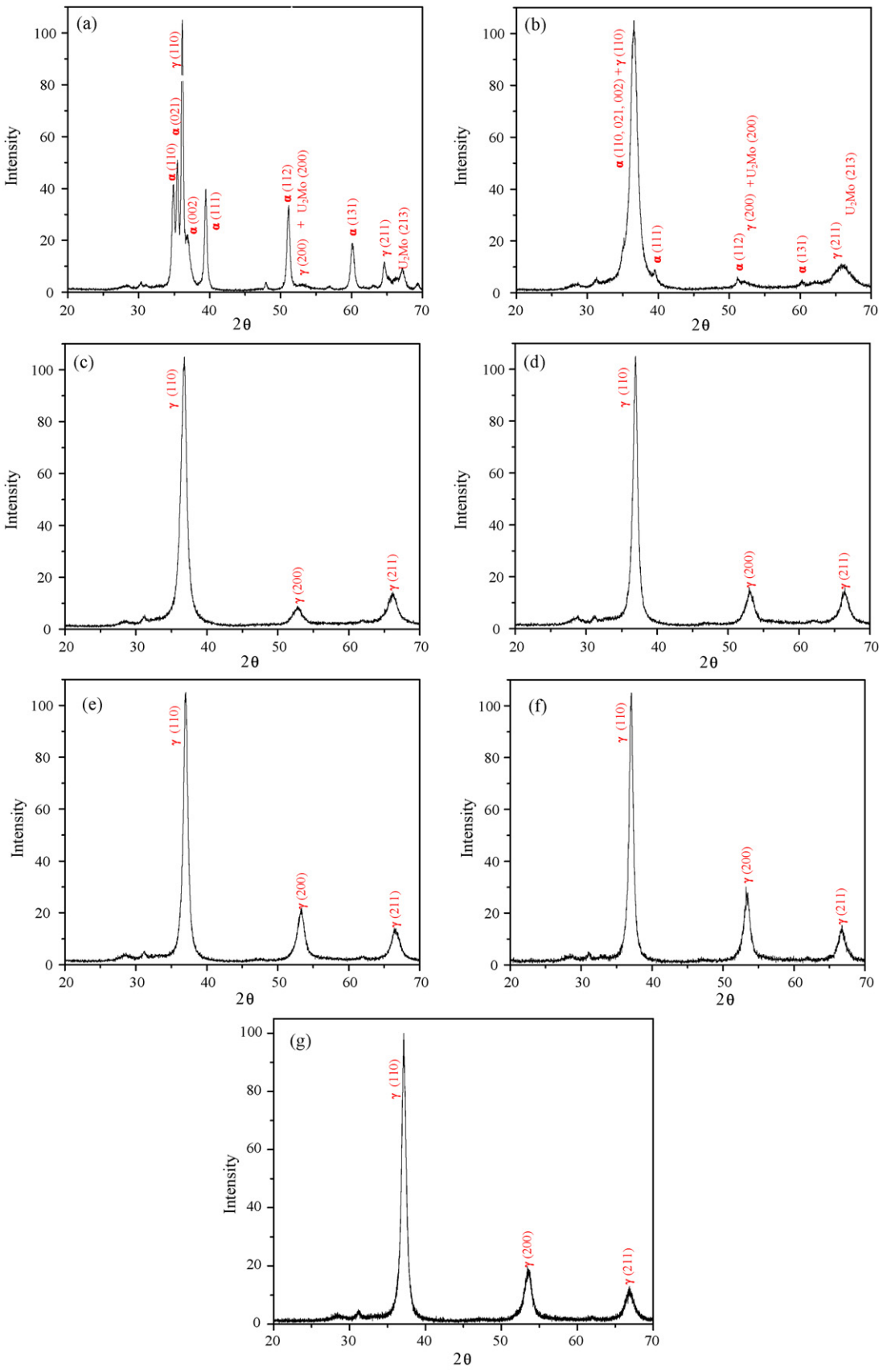

Fig. 4. X-ray diffraction pattern of (a) U–2 wt%Mo alloy, (b) U–5 wt%Mo alloy, (c) U–6 wt%Mo alloy, (d) U–7 wt%Mo alloy, (e) U–8 wt%Mo alloy, (f) U–9 wt%Mo alloy and (g) U–10 wt%Mo alloy.

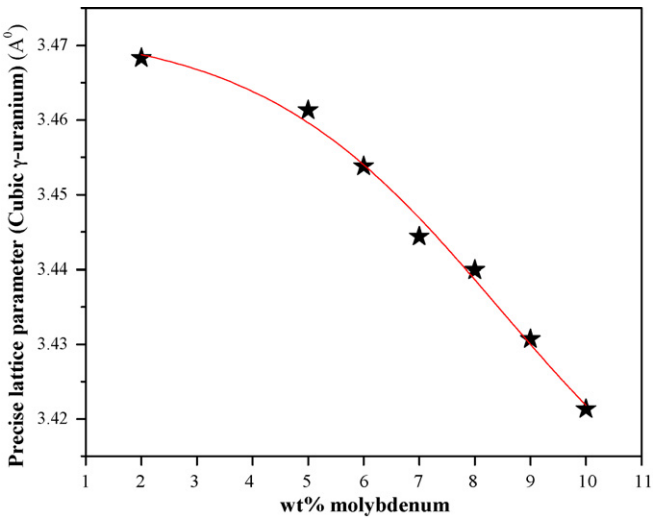

Fig. 5. Precise lattice parameter of cubic γ-uranium with varying amount of molybdenum.

3.1. Phase analysis

The XRD pattern of U–2 wt%Mo alloy (see Fig. 4(a)) clearly indicates that the major phase for this alloy was α-uranium with small amount of γ-uranium and U_2Mo intermetallic compound. The XRD pattern of U–5 wt%Mo alloy (see Fig. 4(b)) and U–6 wt%Mo alloy (see Fig. 4(c)) shows the presence of γ-uranium as major phase with very small amount of α-uranium and U_2Mo intermetallic compound. The XRD pattern of U–7 wt%Mo alloy (see Fig. 4(d)), U–8 wt%Mo alloy (see Fig. 4(e)), U–9 wt%Mo alloy (see Fig. 4(f)) and U–10 wt%Mo alloy (see Fig. 5(g)) shows the only phase present in the all the alloy systems is cubic γ-uranium with no other phase which means either the second phase is in such a small quantity that the XRD equipment is not able to detect it or 100% cubic γ-uranium has been retained at room temperature with molybdenum addition. There was no oxide and carbide peak in any of the XRD patterns which shows that neither oxygen nor carbon was picked up during the alloy preparation.

3.2. Precise lattice parameter calculation

CELREF programme was used for the calculation of precise lattice parameter of cubic γ-uranium unit cell for each U–Mo alloy. The programme uses method of least squares to determine for cell refinement [22]. The precise lattice parameter thus calculated has been plotted against weight percentage of molybdenum in U–Mo alloy (see Fig. 5). The points were fitted using sigmoidal model with the assumption that the curve may be described quantitatively by the three parameter sigmoid function (1), here $X_{1/2}$ is the point of inflection and k is a slope factor (i.e. the change in X corresponding to the most significant change in Y values). The lattice parameter of orthorhombic α-uranium has also been calculated for U–2 wt%Mo and U–5 wt%Mo alloy only because the ($h\,k\,l$) values of α-uranium peaks is not distinctly visible in other U–Mo alloys (see Table 3). The lattice parameter of α-uranium in both U–2 wt%Mo and U–5 wt%Mo alloys does not show any appreciable change since the maximum solid solubility of molybdenum in uranium is 1 at% at room temperature under equilibrium conditions. The slight increase in the lattice parameter of α-uranium for both the U–Mo alloy compositions is due to the formation of supersaturated solid solution of molybdenum in α-uranium.

$$Y = 10 + \left\{ \frac{8}{(1 + \exp((X - X_{1/2})/k)} \right\} \quad (1)$$

3.3. Microstructural analysis using optical microscope

The microstructure of as cast U–2 wt%Mo alloy (as shown in Fig. 6(a)) shows the cellular decomposition and widmanstatten pattern all along the prior gamma grain boundary. During alloy cooling a part of γ-uranium has gone under eutectoid decomposition to form α-uranium and U_2Mo intermetallic which is clearly visible as the lamellar region in the microstructure while there are some region in the microstructure where diffusion has not taken place completely and these are seen as woven basket region (i.e. widmanstatten pattern). In U–5 wt%Mo alloy the microstructure (as shown in Fig. 6(b)) shows bright region as equiaxed γ-grains with dark gray patches as second phase (i.e. α-uranium plus U_2Mo intermetallic). During alloy cooling majority of γ-uranium has been retained at room temperature while some have gone under eutectoid decomposition to form α-uranium and U_2Mo intermetallic product. Microstructure of U–6 wt%Mo alloy (as shown in Fig. 6(c)) shows further increase in γ-uranium phase fraction while some dark patches can be seen as the eutectoid decomposed product of α-uranium and U_2Mo intermetallic. The microstructure of U–7 wt%Mo alloy (as shown in Fig. 6(d)) shows only few dark regions which are again the phase mixture of α-uranium and U_2Mo intermetallic while a substantial region can be seen as γ-uranium. The microstructures of U–8 wt%Mo alloy (as shown in Fig. 6(e)), U–9 wt%Mo alloy (as shown in Fig. 6(f)) and U–10 wt%Mo alloy (as shown in Fig. 6(g)) have shown only equiaxed grains of γ-uranium and there is no second phase visible in it. Microstructures of U–9 wt%Mo alloy and U–10 wt%Mo alloy can be seen as three dimensional since the image was taken in DIC mode. This clearly indicates that as per the microstructure 100% γ-uranium phase can be retained at room temperature with the addition of minimum 8 wt% molybdenum in uranium.

3.4. Image analysis

The quantitative image analysis was carried out using metal work station programme to determine the quantity of different phases in U–Mo alloy ingot samples. The metal work station programme is based on the method described as per ASTM E562 standard for quantitative phase analysis. In the image analysis the α-uranium and U_2Mo intermetallic phase mixture was considered as one phase (since α-uranium and U_2Mo intermetallic was formed due to the eutectoid reaction and they are present in the microstructure as either lamellar decomposed product or widmanstatten) and γ-uranium as second phase. Image analysis was carried out by averaging 15 results at different sections of microstructures for each U–Mo alloy composition. The quantity of γ-uranium versus wt% molybdenum in U–Mo alloy plot is shown in Fig. 7 which clearly indicates the retention of 100% γ-uranium at room temperature with minimum 8 wt%Mo addition to uranium. Sigmoidal model was used to fit the points with the assumption that the curve may be described quantitatively by the three parameter sigmoid function (2), here $X_{1/2}$ is the point of inflection and k is a slope factor (i.e. the change in X corresponding to the most significant change in Y values).

$$Y = 10 + \left\{ \frac{8}{(1 + \exp((X - X_{1/2})/k)} \right\} \quad (2)$$

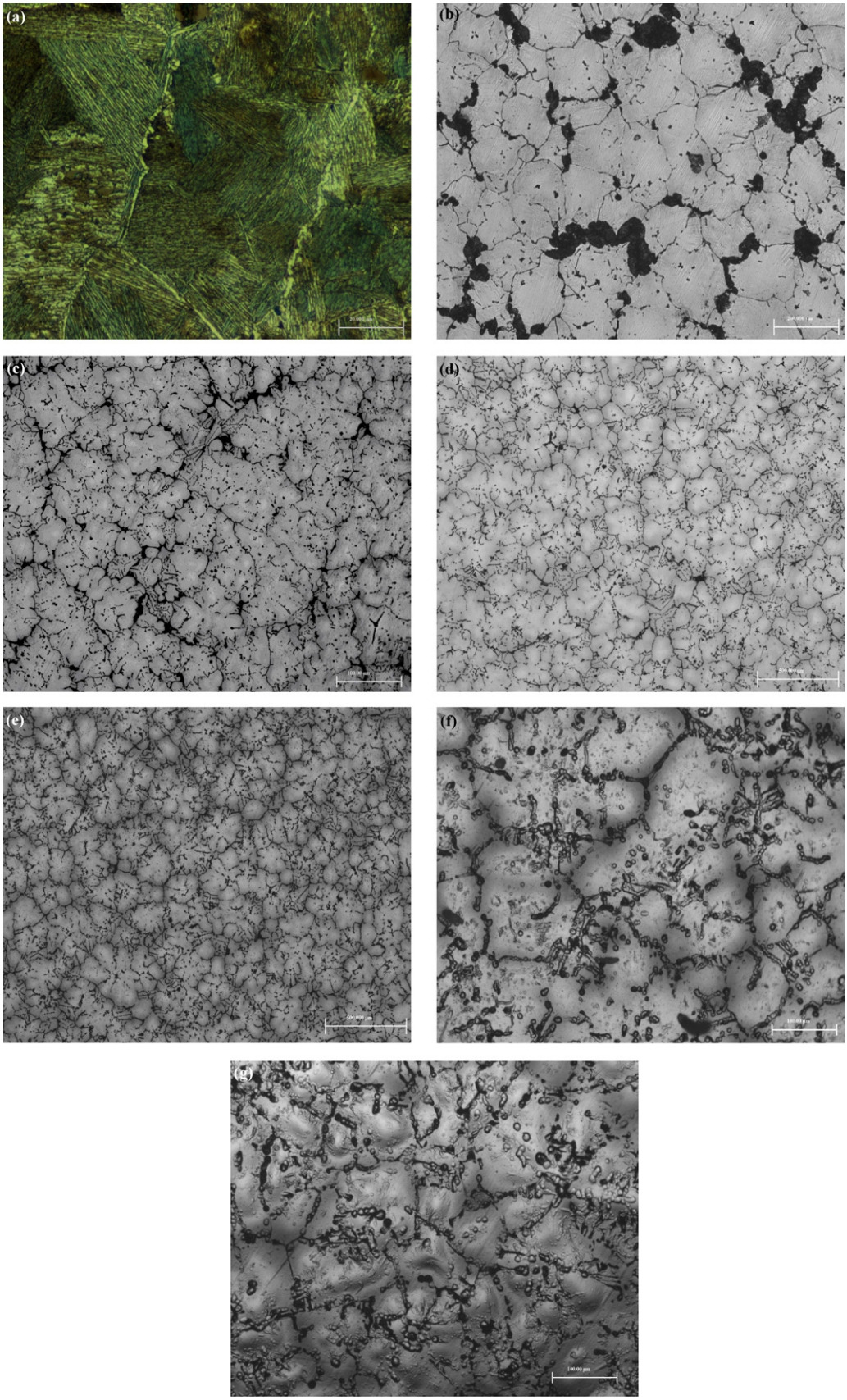

Fig. 6. Microstructures of (a) U–2 wt%Mo alloy, (b) U–5 wt%Mo alloy, (c) U–6 wt%Mo alloy, (d) U–7 wt%Mo alloy, (e) U–8 wt%Mo alloy, (f) U–9 wt%Mo alloy and (g) U–10 wt%Mo alloy.

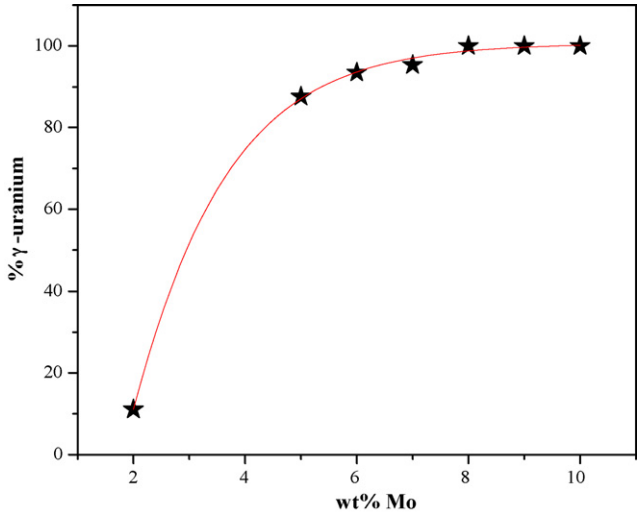

Fig. 7. Quantity (in vol%) of cubic γ-phase at different molybdenum content in uranium.

4. Conclusion

From the experiments and results obtained it can be concluded that though the maximum solid solubility of molybdenum in γ-uranium is 19.8 wt% at 580 °C the minimum quantity of molybdenum required to metastabilize cubic γ-uranium at room temperature is 8 wt% under furnace cooling. XRD results have shown the retention of 100% γ-uranium even with U–6 wt%Mo alloy at room temperature but subsequent examination of microstructure have shown that α-uranium phase and U_2Mo intermetallic will completely disappear only with minimum addition of 8 wt%Mo. Molybdenum atoms replaces uranium atoms from their lattice position during U–Mo alloy preparation (since molybdenum forms substitutional solid solution with uranium). Hence the decrease in lattice parameter of cubic γ-uranium can be seen with the increase of molybdenum content in uranium. During U–Mo alloy preparation α-uranium was supersaturated with molybdenum hence no appreciable change in the lattice parameter of α-uranium was observed when the molybdenum content was increased from 2 wt% to 5 wt%. The change in the lattice parameter of α-uranium with molybdenum addition was also very small because the solid solubility of molybdenum in α-uranium is very low (i.e. 1 at% at room temperature under equilibrium conditions). U–Mo alloys were prepared in an induction furnace under well controlled furnace atmosphere and extreme care was taken during melting to avoid any considerable pick up of oxygen and nitrogen which is evident as the alloys have not shown any appreciable change in weight.

Acknowledgements

The authors are grateful to Messrs. Amit Sharma and M.I. Shaikh, Atomic Fuels Division, BARC for machining uranium metal pieces in the required dimension. The authors also express their sense of gratitude to Mr. R.P. Singh, Associate Director, Nuclear Fuels Group, BARC for providing necessary support of their facility as and when needed.

References

[1] R.F. Domagla, T.C. Wiencek, H.R. Tresh, Nucl. Technol. 62 (1983) 353.
[2] J.P. Durand, Y. Fanjas, Proceedings of the 16th International Meeting on Reduced Enrichment for Research and Test Reactors, Japan Atomic Energy Research Institute Report, Oarai, Japan, JAERI-M 94-02, 1994, pp. 71–78.
[3] J.P. Durand, P. Laudamy, K. Richter, Proceedings International Meeting on Reduced Enrichment for Research and Test Reactors, 18–23 September, Argonne National Laboratory Report, ANL/RERTR/TM-20, Williamsburg, 1994.
[4] V.P. Sinha, G.J. Prasad, P.V. Hegde, R. Keswani, C.B. Basak, S. Pal, G.P. Mishra, J. Alloys Compd. 473 (2009) 238.
[5] G.L. Hofman, R.F. Domagala, G.L. Copel, J. Nucl. Mater. 150 (1987) 238.
[6] M. Ugajin, A. Itoh, M. Akabori, N. Ooka, Y. Nakakura, J. Nucl. Mater. 254 (1998) 78.
[7] M.K. Meyer, T.C. Wiencek, S.L. Hayes, G.L. Hofman, J. Nucl. Mater. 278 (2000) 358.
[8] A.N. Holden, Physical Metallurgy of Uranium, Addison-Wesley Publishing Co. Inc., USA, 1958.
[9] ASM International, Properties and Selection: Non Ferrous Alloys and Special-Purpose Materials, vol. 2, 1965–1994.
[10] G.L. Hofman, M.K. Meyer, RERTR Conference, October 18–23, 1998, Sao Paulo, Brazil, 1998.
[11] V.P. Sinha, P.V. Hegde, G.J. Prasadm, H.S. Kamath, 17th Plansee Seminar, vol. 1, Reutte, Austria, 2009 (RM 78/1-16).
[12] R.L. Craik, D. Birch, C. Fizzotti, F. Saraceno, J. Nucl. Mater. 6 (1962) 13.
[13] M.K. Meyer, C.L. Trybus, G.L. Hofman, S.M. Frank, T.C. Wiencek, Proceedings of the 1997 International Meeting on Reduced Enrichment for Research and Test Reactors Argonne National Laboratory Report, 1999, p. 81 (ANL/TD/TM99-06).
[14] C.L. Trybus, T.C. Wiencek, M.K. Meyer, D.J. McGann, C.R. Clark, Proceedings of the 20th International Meeting on Reduced Enrichment for Research and Test Reactors Argonne National Laboratory Report, 1999, p. 19 (ANL/TD/TM99-06).
[15] J.-S. Lee, C.-H. Lee, K.H. Kim, V. Em, J. Nucl. Mater. 280 (2000) 116.
[16] B.W. Howlett, J. Nucl. Mater. 35 (1970) 278.
[17] A.G. Harding, M.B. Waldron, UKAEA (Harwell Report, AERE M/R-2673), Part 1, 1958.
[18] J. Lehmann, C.R. Acad. Sci. (Paris) 248 (1959) 2098.
[19] K. Tangri, G.I. Williams, J. Nucl. Mater. 4 (1961) 226.
[20] V.P. Sinha, G.P. Mishra, S. Pala, K.B. Khan, P.V. Hegde, G.J. Prasad, J. Nucl. Mater. 383 (2008) 196.
[21] V.P. Sinha, P.V. Hegde, G.J. Prasad, G.P. Mishra, S. Pal, Trans. Indian Inst. Met. 61 (2) (2008) 1–6.
[22] B.D. Cullity, Elements of X-ray Diffraction, Addison-Wesley Publishing Co. Inc., USA, 1989, pp. 360–363.